THE SAN BERNARDINO VOLCANIC FIELD OF SOUTHEASTERN ARIZONA*

D. J. LYNCH
Laboratory of Isotope Geochemistry
Department of Geosciences
University of Arizona
Tucson, Arizona

INTRODUCTION

The San Bernardino volcanic field, a late Cenozoic, multivent basaltic volcanic field, occupies the northern third of San Bernardino Valley in southeastern Cochise County, Arizona, and adjoining parts of Hidalgo County, New Mexico and Sonora, Mexico (fig. 1). The volcanic features are scattered across the valley floor and onto the flanks of the Peloncillo Mountains to the east and the Perilla, Pedregosa and Chiricahua mountains to the west. The extensive lava flow in the Animas Valley to the east, beyond the Peloncillo Mountains, is related to this field because of its proximity, chemistry and age.

GEOLOGIC SETTING

Paleozoic and Mesozoic sedimentary rocks of the region were deformed during the Laramide orogeny such that attitudes of some exposed sedimentary beds of the Pedregosa Mountains are vertical or overturned. Two major thrust faults are found where Paleozoic rocks have been thrust southward over Cretaceous rocks; one at Limestone Mountain and the other north of U.S. Highway 80 where the road passes out of the valley westward towards Douglas. Thick rhyolite flows erupted around 25 m.y. ago, have buried a topography eroded on the deformed older rocks (Marjaniemi, 1969; Shafiqullah and others, this guidebook).

Basin and Range structure and physiography is especially well displayed in the San Bernardino volcanic field and vicinity. The graben-valleys containing most of the volcanic features are bounded by horst-mountain blocks of the Perilla-Pedregosa-Chiricahua mountains on the west and the Peloncillo Mountains on the east. The southern end of San Simon Valley adjacent to the San Bernardino volcanic field is perhaps the most classic graben in the entire area. On both sides of this valley, the mountain spurs terminate in distinct, straight lines. Along the Chiricahua Mountains flank, the spurs terminate in triangular facets which stand above alluvial fans active at the mountain front. While deposition at the mountain front may occur as a result of climatic factors, trenching of alluvial deposits in canyon mouths suggests a tectonic cause. Along the front of the Peloncillo Mountains, evidence for recent movement is lacking; fan heads are trenched and active deposition is taking place further down the fans toward the center of the valley.

Profiles of the residual Bouguer gravity anomaly show that the graben bounding faults are situated along the mountain fronts (Lynch, 1973). A steep gravity gradient delineates the southern end of San Simon Valley about 3 km south of Apache, Arizona. No surface feature reflects this termination on the valley floor, but the mountain fronts are offset at this place, 5 km on the Peloncillo side and 10 km on the Chiricahua side (fig. 1).

Structural relationships in the San Bernardino Valley are not as simple. This valley is almost twice the width of San Simon Valley to the north (fig. 1), and the gravity profile is asymmetrical with a maximum along the west side. Isolated limestone outcrops found near the center of the valley are also indicators of sub-surface structural complexity. Dense basalts of indeterminate thickness complicate the gravity analysis but there are two possible structural models. Either the basin
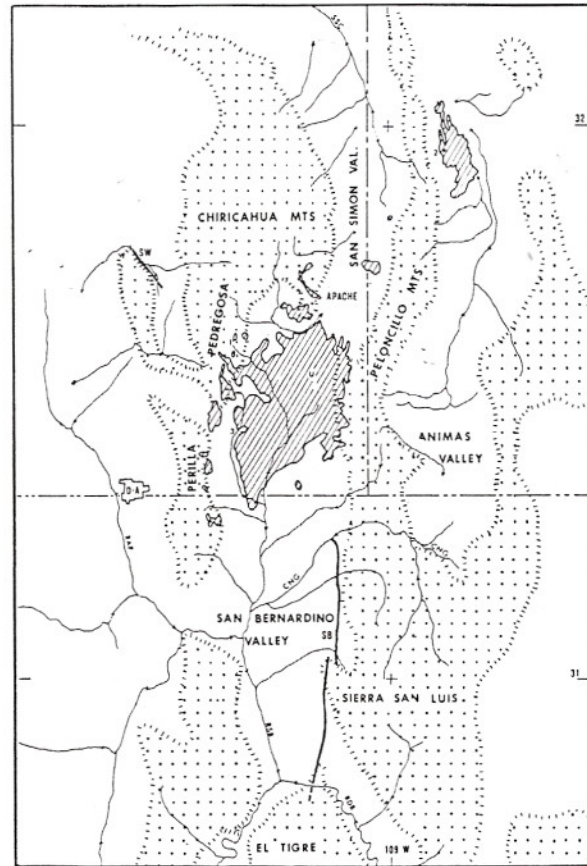

Figure 1. Regional setting of San Bernardino volcanic field. Hachures mark the break in slope between valley floors and mountains (stipple). Cross hatching shows area covered by basalts of San Bernardino volcanic field; the numbers are dated samples (Table 2). Stream flow direction is indicated by arrow heads: (SSC) San Simon Creek; (RAP) Rio de Agua Prieta; (RDB) Rio de Bavispe; (CNG) unnamed river of Cienaguita Ranch. Heavy solid lines mark recent fault scarps: (SW) Swisshelm; (SB) 1887 San Bernardino scarp. (D-A) is Douglas-Agua Prieta.

block is tilted toward the west or the western parts of the basin have been faulted downward relative to the eastern parts along buried faults parallelling the margin of the valley. Alignments of volcanic cones parallel to bounding faults lend support to the second model.

South of Guadalupe Canyon and the southernmost basalt flows in Mexico, the eastern fault is marked by a spectacular vertical scarp created by the earthquake of May 4, 1887 (Aguillera, 1888; Sumner, 1977). The scarp extends half the length of the valley from this point to its termination in the Sierra El Tigre to the south. At its highest, the scarp is over 4 m high. North of Pitaicachi, the scarp parallels or follows an old fault contact between folded Paleozoic limestones to the east and valley-fill sediments to the west, showing this to be a continuation of Basin and Range faulting.

The western basin boundary fault may not be a single, contiguous feature. Three en echelon faults intersect the physiographic basin margin at about a 25 degree angle and occur at intervals of 3-4 km. A fourth fault is sub-parallel to the other three. The sense of motion for these faults (downward on the eastern side) is consistent with an interpretation of these as basin-margin faults.

DRAINAGE

Drainage patterns are good indicators of tectonic activity. The basins on either side of San Simon Valley are closed, draining internally to large playas. Although the San Simon drainage is integrated into the Gila River system, the stream gradient is shallow enough (3.6 m per km) that sediment is accumulating in the valley and very little is carried out of the valley by the axial stream. In contrast, the Rio San Bernardino, with a gradient of nearly 8 m per km, is cutting headwards and transporting sediments down the valley.

The overall regional drainage pattern is superimposed on topography (fig. 1). Rio San Bernardino flows southward out of the valley through a narrow defile where it joins the Rio de Bavispe which enters the southern San Bernardino Valley through a canyon cut through the Sierra El Tigre, rather than down the axis of the valley. Cieneguita Creek is more striking as it rises on the east side of the Animas Valley, flows westward across the southern end of the valley, passes through the Peloncillo Mountains and into the San Bernardino Valley, where the creek has cut a deep barranca in an old, flat erosional surface.

These patterns suggest that recent tectonic activity has adjusted base level and caused renewed downcutting by the streams in some areas. Prior to this activity, relief may have been relatively low and streams probably "wandered" between low hills and across the grain of modern topography. Uplift has subsequently entrenched many of the old stream courses.

VOLCANIC FEATURES

Pyroclastic cones are the most prominent features of this volcanic field; their relatively good state of preservation attests to the young age of the field. Almost all of the cones are constructed of agglutinate, i.e., welded spatter (fig. 2). Lava flows associated with the cones are usually of limited extent, covering only a few square kilometers. Agglutinate cones of the San Bernardino field are layered and the sides of eroded cones are stepped. The layers range in coherence from loose fragments to solid, rootless flows.

Figure 2. Agglutinate cones in southern San Bernardino volcanic field. Spines and festoon flow-banding remnant on the lava flow in the foreground identify it as the youngest in the field.

San Bernardino volcanic field lacks any fresh volcanic features like those in the San Francisco Peaks volcanic field at Sunset Crater and the Bonita flow. Festoon flow banding and lava spines are remnant on the youngest flow at Cinder Hill (fig. 2), but the rock surfaces are deeply weathered and the flow top is approaching the flat featurelessness of the other lava flows in this field.

Some of the younger lava flows of the San Bernardino field have uneroded margins, and their original extent can be defined (see fig. 5). Most of the others are at least partially eroded or buried beneath sediments in the valley. Basalt flows constitute an important part of the modern basin fill. A water well in the center of the valley penetrates seven lava flows and terminates in an eighth. Another deep well 3 km distant penetrates six lava flows, but there is no correlation between the flows of the two wells. The most deeply eroded lava flows are those on the flanks of the mountains on either side of the valley (figs. 3, 4). The tectonic implications of these flows are discussed below. In all but a few places, source vents of the older flows are eroded away and can no longer be found.
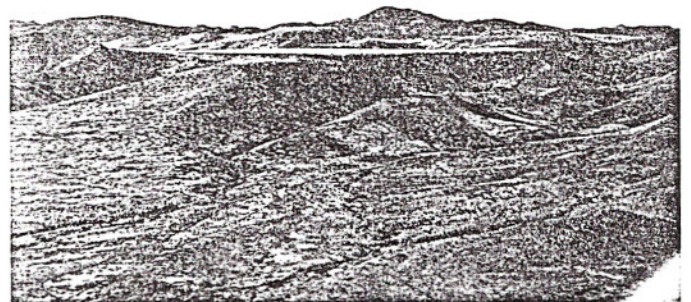

Figure 3. Older basalt flow remnant on west side. This mesa north of the Joe Glenn ranch is pediment covered by two lava flows; the lowest has an age of 3.0 ± 0.12 m.y. The rhyolite cliff in the background is the only possible source for rhyolite in the gravel layer which separates the lava flows.

Figure 4. Basalt flow remnants on east side. These flow remnants, less extensive than the flows of Figure 3, are at the same elevation, 5600 ft.

Figure 5. Steam-blast eruption features of the San Bernardino volcanic field. "C" shaped Krentz Ranch tuff ring lies around the source of a 5.4 km-long lava flow which the road crosses. The cone immediately to its left is Stop 2 of the First Day Road Log. Paramore Crater is the prominent crater directly down from the lava flow near the bottom of the photograph. Another, unnamed tuff ring which contains a large playa can be seen to left of Paramore near the left edge of the photo. Directly below Paramore and partially off the photo is another "C" shaped tuff ring. The white areas left of this are limestone outcrops. Arrows show north (Photograph courtesy of NASA).

TUFF RINGS AND MAAR CRATERS

Steam-blast eruptions occurred in at least five places in the San Bernardino volcanic field. Features created by these atypical eruptions are distinctive maar craters, depressions blasted into the land surface, tuff rings, and broad, low profile "cones" of mixed chilled-lava and detritus from the eruption site. Only two actual maar craters are found in the field, both of them about 60 m deep and surrounded by tuff rings. Paramore Crater (fig. 5) is oval, 1 by 1.5 km in size, and is situated between agglutinate cones. The other, unnamed, maar crater is circular and 1 km in diameter (fig. 6). Three "C" shaped tuff rings, without central maar craters, are other distinctive steam-blast features. Dunes, anti-dunes, reverse graded bedding, truncated and scoured cross beds are all found in tuff ring deposits of the San Bernardino volcanic field (fig. 7). Some beds have a fine laminar bedding while others have layers of completely unsorted fragmental material (fig. 8).

Steam-blast explosions lifted fragments of older basalt flows and underlying rock along with the unconsolidated detrital material out of the craters. The larger fragments were projected as ballistic blocks and impacted the soft tuff leaving impact craters at the point of contact. One such rhyolite ballistic block found in the tuff on the northern side of Paramore Crater is almost 2 m in the largest dimension (fig. 9). Several others of smaller size have been found in the vicinity as well as rounded limestone "loaves," 0.5 m along the major axes. There is neither evidence for nor reason to expect a shallow magma chamber under these craters from which magma could withdraw to initiate their collapse.

Fine-grained, laminar tuff beds are common around Paramore Crater (fig. 7) and the other unnamed maar crater, while the other three "C" shaped tuff rings have coarser tephra beds (fig. 8). There appears to be a continuous series of "phreatomagmatic" (water-modified lava) deposits ranging from the fine-grained laminar material of the maar-associated tuff rings to a palagonitic basalt agglomerate such as that constituting the small subsidiary cone south of the Tex Canyon road (Stop 2, First Day Road Log). The palagonite, or hydrated basaltic glass, is the factor linking the relationship between these two types of deposits.

PETROLOGY AND PETROGRAPHY

The San Bernardino basalts are basanites, similar in texture and composition to contemporaneous basanitic basalts from other parts of the Basin and Range and surrounding provinces. They are noteworthy for the large amount of xenolithic material they contain, including large lherzolite and pyroxenite nodules of probable mantle provenience. Megacrysts of plagioclase, pyroxene, amphibole and spinel are common. In this aspect, the field is not unlike Periodot Mesa near San Carlos (Wohletz, 1978) or some parts of the San Francisco Peaks volcanic field near Flagstaff (Stoesser, 1974).

Table 1 lists compositions of some selected San Bernardino basalts along with published average basalt compositions from the literature. San Bernardino basalt compositions are similar to Leeman and Rogers' (1970) average alkali olivine basalts from the Basin and Range province and to the worldwide average alkali olivine basalt defined by Schwarzer and Rogers (1974). The only difference is a somewhat higher content of alkali oxides in the San Bernardino flows.

Textures of the flow rocks range from microcrystalline trachytic to aphanitic ophitic and sub-ophitic. In the quickly

Figure 6. Panorama of the southern maar crater. Layers seen in the walls are thin lava flows and detrital material of the valley fill in which this crater was blasted by steam-blast eruptions. Like Paramore Crater, this maar has a playa in its center but no lava flow was thi.

cooled flows, the plagioclase laths are flow aligned and very small. In the more slowly cooled flows, the groundmass plagioclase crystals are larger, up to 2 mm, randomly oriented and enclosed by pyroxene and glass in a sub-ophitic texture. All of the flows examined are porphyritic and megacrysts (phenocrysts more than 100 times larger than groundmass crystals) are abundant. Weathering of the lavas, particularly the scoriaceous material, has disaggregated megacrysts from the groundmass, and such megacrysts may be found in some places scattered on the ground.

Plagioclase occurs as the most abundant groundmass constituent and phenocryst. Groundmass compositions range from calcic oligoclase (An-30) to labradorite (An-55) while the phenocrysts are predominantly labradorite. Sieve texture is common in both phenocrysts and megacrysts. A few of the megacrysts found have crystal faces but no sharp edges; cross sections through the crystals are more oval than polygonal. These megacrysts are either translucent or transparent with a white to honey-yellow color and some exhibit conchoidal fracture. Groups of parallel bubbles are found in many of the megacrysts but none in sectioned phenocrysts. Gutmann (1974) proposed that these "tubular voids" resulted from bubbles of CO_2 adhering to and "poisoning" the faces of the growing crystal. As the crystal grew, the bubbles increased in size only in an outward direction.

Pyroxene, the second most abundant mineral, is slightly subordinate to plagioclase as a groundmass mineral but much more abundant as megacrysts and crystalline aggregate nodules. Orthopyroxene occurs sparsely, while the clinopyroxene has a composition similar to that of augite. One of the megacrysts analyzed had 8.8% Al_2O_3, which suggests crystallization in an environment where jadeitic pyroxene is stable. Megacrysts are shiny black and their poor cleavage, glassy lustre and conchoidal fracture promotes misidentification as obsidian. Crystals occurring in the crystalline aggregate pyroxenite nodules exhibit better cleavages and a less glassy

lustre than the megacrysts. Some megacrysts are oikocrysts which contain inclusions of euhedral spinel octahedra or subhedral olivine crystals. Tubular voids are also found in pyroxenes but not as commonly as in plagioclase. One megacryst had three intersecting sets of parallel voids.

Olivine is less abundant than pyroxene and occurs as a minor groundmass mineral and as large phenocrysts. Unlike the San Carlos vent, rocks of the San Bernardino field contain no olivine megacrysts. Almost all phenocrysts are altered to iddingsite along grain boundaries and fractures. One lava flow near Skeleton Canyon contains olivine altered to the much less common, green bowlingite. Only a few of the phenocrysts sectioned were euhedral and none were embayed. No reaction rims were observed.

Figure 7. Thin laminar tuff layers at Paramore Crater. Dunes and anti-dunes can be seen in this outcrop. Below the tuff layers is eroded agglutinate from an older cone. The inclination is initial dip.

Bower Crater

...gh to support a vertical wall. Around it are scattered agglutinate cones, and old remnant lava flows can be seen on the flanks of the ...cillo Mountains in the background.

Lherzolite nodules, aggregates of olivine and chrome diopside with minor spinel, are abundant in many parts of the volcanic field. A few are layered with pyroxene-rich zones. Although textures observed in the nodules were not unequivocally cumulate, the layering and lack of any metamorphic deformation suggests that the lherzolites were of cumulate origin.

Spinels occur as the most common accessory minerals. Phenocrysts and megacrysts exhibit a great compositional range in which aluminum, titanium, magnesium and chromium freely substitute for iron. Magnitite, spinel, hercynite, ulvospinel and magnesio-chromite were specifically identified by x-ray diffraction. The aspect of the octahedral crystals is unusual as well. Points and edges are commonly sharp while the faces are often embayed and some free megacrysts are skeletal.

Amphibole, the least common mineral, occurs only as megacrysts and in crystalline aggregate nodules. The most common type of amphibole is kaersutite, a titanium-rich basaltic-hornblende. The crystals have the same outward appearance as the shiny black pyroxenes but the obvious amphibole cleavage, perfect in two directions, allows easy identification. Kaersutites, like pyroxenes, have included bubbles but the parallel groups observed in some of the other minerals have not been found.

Minor accessory minerals include calcite, which occurs both as vesicle fillings and as interstitial masses which appear to be part of the rock fabric. Zeolites are found in some places in vesicles and in fractures covering the rock surfaces. Zeolites form the white specks observed in many exposures. Phlogopite and nepheline have been reported by Evans and Nash (1978).

ORIGIN OF THE BASALTS

Alkali-olivine basalts originate through partial melting of mantle materials and rise through the crust without contamination. Evans and Nash (1978) investigated compositions of co-existing mineral pairs from the San Bernardino volcanic field and used thermodynamic calculations to compute temperatures and pressures of equilibrium. Solutions for the source region were "1400°C and 21 kb, equivalent to a depth of 67 kilometers" (Evans and Nash, 1968). They have suggested that any local magma chambers should be located at a depth of 33 km, beneath the presumed crust-mantle boundary.

Whole-rock major element chemical analyses have been made on lava flows from widely separated points in the field; representative analyses are listed in Table 1 along with radiometric ages from Table 2. There is no discernable variation in major element chemistry of these rocks which can be related either to position or age.

Schwarzer and Rogers (1974) propose that alkali olivine basalt is a primary magma-type generated in a variety of tec-

Figure 8. Coarse tuff in the walls of the unnamed maar crater. Poor sorting and crude bedding in this steam-blast deposit probably indicate a lower energy depositional environment than seen in Figure 7.

Figure 9. Ballistic block at Paramore Crater. This nearly 2 m rhyolite boulder is in tuff deposits on the north side of Paramore Crater. It came from a rhyolite layer in the bedrock under the crater, lifted out of the eruption site by the power of the steam explosions.

tonic settings at sufficient depth in the upper mantle to be unaffected by the nature of the overlying crust, be it continental, oceanic or island arc. Basalt major-element composition is neither affected by possible variations in mantle composition in these settings nor by passage of the magma through the crust. Sun and Hanson (1975) suggest that alkali olivine basalts are derived from the deep, isolated mantle below their proposed zone of modern convection. However, Gill (1976) suggested that different types of basalt are generated from a chemically homogeneous mantle by differing temperature, total pressure, partial pressure of water, fugacity of oxygen and heat flux, all of which control the degree of partial melting.

If magma genesis occurs at depths in excess of the thickness of the crust, local disturbances of the crust such as basin-margin faulting will have no effect on the process. Basaltic volcanism appears to be contemporaneous with renewed subsidence of the northern San Bernardino Valley which leads to speculation that these two effects may be related. This is unlikely considering the conclusions of Schwarzer and Rogers (1974) as well as the observed relations of the basalts to the valleys. The Animas flow in the tectonically stable Animas Valley belongs to the group. Only a few flows are found in the active San Simon graben and none are found in the recently active southern San Bernardino Valley. While basin subsidence is the main feature of the Basin and Range province, alkali-olivine basalt volcanos are not common and only three groups are large enough to be called volcanic fields.

AGES OF VOLCANISM

Four radiometric ages on basalts of the San Bernardino volcanic field fall within the late Pliocene or Pleistocene Epochs. The youngest flow with an age of 0.274 ± 0.050 m.y. (no. 3) shows that little more than 300,000 years is necessary to remove original flow top features. The surface of the Animas basalt flow, 0.544 ± 0.050 m.y. (no. 2) is eroded flat. The Animas flow, remote from the main volcanic field, is the only flow from a fissure eruption, and it has no pyroclastic cone at its source.

An age of 0.975 ± 0.100 m.y. was determined on the lava flow which supports the south wall of Paramore Crater (labeled "U," fig. 1; Marvin and others, this guidebook). The surface of this lava flow had been weathered and eroded flat prior to the Paramore steam blast eruption.

The oldest date on a Bernardino basalt was determined on the dissected lava flow shown in Figure 3. This age of 3.30 ± 0.12 m.y. (no. 1) bears on the rate of erosion in the area and allows some speculations to be made concerning the development of the valley.

EVOLUTION OF SAN BERNARDINO VALLEY

Lava flow remnants form distinctive tables at essentially the same elevations along the flanks of the mountains on both sides of the northern San Bernardino Valley (figs. 3, 4). The basalt appears to have flowed out onto pediments or alluvial embayments in mountain fronts of much lower relief relative to the valley floor than is present today. Modern lava flows from conduits in these mountains are confined to canyons, spreading only after reaching the valley floor. Topography in the not too distant past was subdued.

This kind of topography presently exists in the Animas Valley. The Animas Valley floor is 150 m higher than the San Bernardino Valley floor and the mountain front between this valley and the Peloncillo Mountains is convoluted with the kind of alluvial embayments preserved beneath the older San Bernardino flow remnants.

Two lava flows are found on the mesa north of the Joe Glenn ranch (fig. 3). The lowest is the oldest dated rock (Table 2, no. 1). These flows are separated by 2 m of alluvium which contain cobbles of pink rhyolite. The only possible source for this rhyolite, an outcrop higher than the mesa, is now separated from the mesa by two canyons 70 and 100 m deep. Depth/time erosion rates of 20 and 30 m per m.y., based on the 3.3 ± 0.1 m.y. age of the lowest flow, are probably high since both canyons are developed along faults showing post-3 m.y. old movement.

Basaltic volcanism began in the San Bernardino Valley in excess of 3 m.y. ago when the northern part of the valley looked much like the modern Animas Valley. Renewed subsidence, which probably began not long after volcanism, lowered the valley floor relative to the mountains. The basin thus created was filled with layers of detritus separated by basalt flows. This subsidence left the older lava flows as remnants in the hills flanking the valley.

Superposition of regional drainage probably resulted from the same tectonic causes responsible for subsidence of the valley. Preservation of the Animas Valley in its eroded state sug-

Table 1. Chemistry of basalts from San Bernardino volcanic field (in percent)

	Worldwide Average AOB[a]	Basin & Range AOB[b]	(1) BVF-1	(2) BVF-148	(3) BVF-91	(4) BVF-104	(5) BVF-20
SiO_2	46.7 ± 1.9	48.5	47.4	45.1	49.7	45.9	48.0
Al_2O_3	15.1 ± 1.4	15.1	15.7	16.8	15.2	15.3	16.4
Fe_2O_3	13.0 ± 1.4	10.1	11.6	10.6	10.4	11.6	11.3
MgO	7.7 ± 1.9	7.5	7.7	7.2	8.3	9.4	6.7
CaO	9.9 ± 1.2	9.5	9.1	9.0	10.0	9.3	11.3
NaO_2	3.2 ± 0.4	3.5	3.1	4.6	3.0	3.7	4.6
K_2O	1.2 ± 0.4	1.5	1.2	1.8	0.8	1.8	2.1
TiO_2	2.7 ± 0.7	1.8	2.3	1.9	1.8	2.4	2.1
Latitude:			31°3.64'	31°36.6'	31°56.5'	31°26.9'	31°42.0'
Longitude:			109°20.2'	109°08.7'	108°53.3'	109°17.5'	109°15.9'
Age Million Years: (see Table 2)			3.30	0.975 ± 0.10	0.544	0.274	

Notes:

Atomic Absorbtion Analyses By D. J. Lynch

Precision ± 3% or Better—Total Iron Reported As Fe_2O_3

a. Worldwide average Alkali Olivine Basalt—means and standard deviations, Schwarzer and Rogers (1974).
b. Average Basin and Range Alkali Olivine Basalt—Leeman and Rogers (1970).
1. Mesa north of Joe Glenn Ranch, lower flow
2. South wall Paramore Crater—U.S.G.S. age
3. Animas Valley flow
4. Flow at Cinder Hill, youngest in field
5. Cone (Stop 2, field trip)

Table 2. K-Ar ages of basalts from the San Bernardino volcanic field

Sample No.	Sample description and location	Percent K	Radiogenic argon-40 ($\times 10^{-12}$ mole/g)	Percent atmospheric argon-40	Age in m.y.
1. UAKA 72-61	Whole rock basalt, older Bernardino basalts, lower basalt from the southwest projection of a prominent table north of the Joe Glenn Ranch. Two lava flows are separated by 2 m of rhyolite cobble gravel. Altitude 5600 ft, Pedregosa Mountains, Cochise Co., Arizona. Lat. 31° 36.43' N Long. 109° 20.22' W.	1.05	6.01	61.7	3.30 ± 0.12
2. UAKA 74-44	Whole rock basalt, Animas flow, collected from massive flow basalt exposed in the first roadcut east of Antelope Pass on N.M. Highway 9. It has reversed polarity. Animas Valley, Hidalgo Co., N.M. Lat. 31° 56.5' Long. 108° 53.3'.	0.967 0.970	0.925 0.894 0.923	84.9 85.0 78.4	0.544 ± 0.050
3. UAKA 75-109	Whole rock basalt, the youngest Bernardino basalt. Sample from massive basalt on eroded edge of lava flow crossed by access road north of Cinder Hill. Altitude 4190 ft, San Bernardino Valley, Cochise Co., Arizona. Lat. 31° 26.92' N Long. 109° 17.46' W.	1.173 1.182	0.550 0.530 0.600	91.6 91.7 91.5	0.274 ± 0.050

Constants used:

$\lambda_\beta = 4.963 \times 10^{-10}$ yr^{-1}

$\lambda_e = 0.581 \times 10^{-10}$ yr^{-1}

$\lambda = 5.544 \times 10^{-10}$ yr^{-1}

$^{40}K/K = 1.167 \times 10^{-4}$ atom/atom

gests that basin subsidence can be restricted to limited areas and may well be episodic for any particular basin. The 1887 fault scarp is evidence that the Basin and Range disturbance is still in progress in this area.
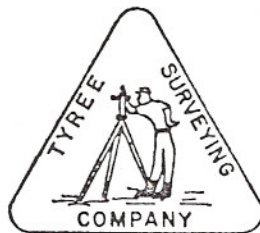
ACKNOWLEDGMENTS

REFERENCES

Aguillera, J. G., 1888, Fenomenos seismicos del 3 de Mayo de 1887: Anales del Ministerio de Fomento de la Republica Mexicana, v. 10.

Evans, S. H., and Nash, W. P., 1978, Quaternary mafic lavas and ultramafic xenoliths from southeastern Arizona [abs.]: Geol. Soc. Amer. Abs. with Programs, v. 10, p. 216.

Gill, J. B., 1976, Evolution of the mantle: geochemical evidence from alkali basalt: Comment: Geology, v. 5, p. 625.

Guttman, J. T., 1974, Tubular voides within labradiorite phenocrysts from Sonora, Mexico: Amer. Mineralogist, v. 59, p. 666-672.

Leeman, W. P., and Rogers, J. J. W., 1970, Later Cenozoic alkali olivine basalts of the Basin-Range province, U.S.A.: Contr. Mineral. and Petr., v. 25, p. 1-24.

Lynch, D. J., 1973, Reconnaissance geology of the Bernardino Volcanic Field, Cochise County Arizona [M.S. thesis]: Tucson, Univ. of Ariz., 101 p.

Marjaniemi, O. K., 1969, Geologic history of an ash flow sequence and its source area in the Basin and Range province of southeastern Arizona [Ph.D. dissertation]: Tucson, Univ. of Ariz., 176 p.

Schwarzer, R. A., and Rogers, J. J. W., 1974, A worldwide comparison of alkali olivine basalts and their differentiation trends: Earth and Planet. Sci. Letters, v. 23, p. 286-296.

Stoeser, D. B., 1974, Xenoliths of the San Francisco volcanic field, northern Arizona: Geology of North Arizona, vol. II, Karlstrom, T. N. V., Swann, G. A., and Eastwood, R. L. (eds.), for Geol. Soc. America, Rocky Mtn. Sec., Flagstaff, Ariz., p. 530-546.

Sumner, J. R., 1977, The Sonora Earthquake of 1887: Bull. Seis. Soc. Amer., v. 67, p. 1219-1223.

Sun, S. S., and Hanson, G. N., 1975, Evolution of the mantle: Geochemical Evidence from Alkali Basalt: Geology, v. 3, p. 297-302.

Wohletz, K. H., 1978, The eruptive mechanism of the Peridot Mesa Vent, San Carlos, Arizona: Guidebook to the geology of central Arizona: Arizona Bur. Geol. and Min. Tech., Special Paper 2, p. 167-170.